

MIT Open Access Articles

In situ High-Field Dynamic Nuclear Polarization-Direct and Indirect Polarization of [¹³C] nuclei

The MIT Faculty has made this article openly available. **Please share** how this access benefits you. Your story matters.

Citation: Maly, Thorsten, Anne-Frances Miller, and Robert G. Griffin. "In situ High-Field Dynamic Nuclear Polarization-Direct and Indirect Polarization of ¹³C nuclei." *ChemPhysChem* 11, no. 5 (April 6, 2010): 999-1001.

As Published: <http://dx.doi.org/10.1002/cphc.200900908>

Publisher: Wiley Blackwell

Persistent URL: <http://hdl.handle.net/1721.1/82069>

Version: Author's final manuscript: final author's manuscript post peer review, without publisher's formatting or copy editing

Terms of use: Creative Commons Attribution-Noncommercial-Share Alike 3.0





Published in final edited form as:

Chemphyschem. 2010 April 6; 11(5): 999–1001. doi:10.1002/cphc.200900908.

***In-situ* High-Field Dynamic Nuclear Polarization – Direct and Indirect Polarization of ^{13}C nuclei**

Thorsten Maly,

Francis Bitter Magnet Lab and Department of Chemistry, Massachusetts Institute of Technology, Cambridge, MA 02139 (USA)

Anne-Frances Miller[†], and **Robert G. Griffin^{*}**

Francis Bitter Magnet Lab and Department of Chemistry, Massachusetts Institute of Technology, Cambridge, MA 02139 (USA)

[†]Prof. Dr. Anne-Frances Miller, Dept. of Chemistry, University of Kentucky, Lexington KY 40506-0055

Keywords

Dynamic Nuclear Polarization; DNP; Dissolution; Solid-State NMR

In a dynamic nuclear polarization (DNP) experiment, the large Boltzmann polarization of a paramagnetic polarizing agent is transferred to surrounding nuclei by microwave irradiation at the electron paramagnetic resonance (EPR) frequency.[1] The initial DNP experiments were performed in the early 50's [2], but until recently the approach was of limited applicability because it was constrained to low magnetic fields due to a dearth of high frequency microwave sources. However, high-frequency (130-660 GHz), high-power microwave sources are now available and improving, and as a result there have been substantial efforts to move DNP to magnetic fields used in contemporary NMR experiments (200–1000 MHz for ^1H). Thus, in the last decade high-frequency DNP has emerged as a valuable method to overcome the intrinsic low sensitivity of liquid and solid-state NMR experiments.[3–5] In particular, with its increased signal intensities, DNP is of significant interest in applications ranging from particle physics [6] to structural biology [4,5] and clinical imaging.[7]

Recent DNP experiments have been directed at enhancing signal intensities in both solid and liquid state NMR spectra. Due to their superior dispersion and resolution, as well as for technical reasons discussed below, both sets of experiments have relied primarily on observation of low- γ spectra such as ^{13}C or ^{15}N . These nuclear species can be polarized either directly ($e^- \rightarrow ^{13}\text{C}/^{15}\text{N}$) or indirectly via ^1H ($e^- \rightarrow ^1\text{H} \rightarrow ^{13}\text{C}/^{15}\text{N}$), the indirect method relying on a Hartmann-Hahn transfer for the $^1\text{H} \rightarrow ^{13}\text{C}/^{15}\text{N}$ step. The purpose of this communication is twofold: (1) to compare the efficiency of the direct and indirect polarization transfers, and (2) to delineate the conditions under which the direct ^{13}C polarization process is most efficient. Our results indicate that direct ^{13}C polarization is optimal under different conditions when compared to the indirect process. For direct polarization, the maximum enhancement occurs on the low-field, rather than the high-field side of the DNP enhancement profile.

^{*}Fax: (+1) 617 253-5405, rgg@mit.edu.

This is likely because of the lower Larmor frequency of ^{13}C and the distribution of spectral intensity in the EPR lineshape. In addition, we find that the time constant for the polarization buildup, τ_B , for the direct ^{13}C polarization process is a factor of ≥ 20 longer when compared to the indirect method. Our data suggest that the origin of this difference is the more rapid spin diffusion in the ^1H reservoir. Thus, there are significant time savings available by polarizing ^1H followed by Hartmann-Hahn transfer to ^{13}C .

A number of papers have established that, under a variety of experimental conditions at high field, the cross-effect (CE) is the most efficient approach to performing DNP. Briefly, depending on the homogenous linewidth (δ) and the inhomogeneous breadth (Δ) of the EPR spectrum of the paramagnetic polarizing agent, in comparison with the nuclear Larmor frequency (ω_{0I}), the DNP process in solids is governed by the solid-effect (SE, $\delta, \Delta < \omega_{0I}$) or the cross-effect (CE, $\Delta > \omega_{0I} > \delta$). [5,8] However, the efficiency of the SE is determined by *forbidden* electron-nuclear transitions that scale as ω_{0I}^{-2} and therefore the enhancements at high magnetic fields (≥ 5 T) are small, ≤ 15 . [9] In contrast, the underlying mechanism of the CE is a two-step process involving two electrons with Larmor frequencies ω_{0S1} and ω_{0S2} , and a nucleus with a frequency ω_{0I} . Initially, the *allowed* EPR transition of one electron is irradiated and nuclear polarization is generated in a subsequent three-spin flip-flop process through transitions such as $|\alpha_{1S}\beta_{2S}\beta_I\rangle \leftrightarrow |\beta_{1S}\alpha_{2S}\alpha_I\rangle$ or $|\beta_{1S}\alpha_{2S}\beta_I\rangle \leftrightarrow |\alpha_{1S}\beta_{2S}\alpha_I\rangle$. [10,11] The maximum enhancement is achieved, when the difference between the electron Larmor frequencies of two spin packets approximates the nuclear Larmor frequency ($|\omega_{0S1} - \omega_{0S2}| = \omega_{0I}$, matching condition). The DNP-enhanced nuclear polarization then disperses throughout the bulk via spin-diffusion. [12] Typically, in high-field *in-situ* DNP experiments, where the polarization and observation of the NMR signal are performed in the same magnet, the ^1H 's are polarized and the DNP-enhanced ^1H polarization is then transferred to ^{13}C in a subsequent cross-polarization step. [13,14] This procedure is used extensively in magic angle spinning (MAS) experiments, and of course requires a double tuned rf coil. In contrast, in *ex-situ* experiments, the ^{13}C nuclei are polarized directly and the sample is usually dissolved and transferred to another magnet for observation of the high-resolution spectrum. One reason for the choice of direct polarization is that the dissolution process and the sample transfer are more conveniently performed in a cavity devoid of rf coils. In either case it is necessary to record the NMR signals as a function of field or frequency in order to determine the parameters for optimal enhancement.

In current DNP experiments the microwave source has a fixed frequency and therefore the profile of DNP enhancement was recorded by sweeping the magnetic field strength. In Figure 1 the DNP enhancement profile, which is closely related to the shape of the EPR spectrum, is shown for indirect ($e^- \rightarrow ^1\text{H} \rightarrow ^{13}\text{C}$), and direct ($e^- \rightarrow ^{13}\text{C}$) ^{13}C polarization. Both profiles were recorded from the same sample ($^{13}\text{C}_3$ -glycerol/ $^2\text{H}_2\text{O}$) using 1-(TEMPO-4-oxy)-3-(TEMPO-4-amino)-propan-2-ol (TOTAPOL) as the polarizing agent. [15] The enhancement profile reveals the typical shape for TEMPO-based polarizing agents [16–18] with field positions for the maximum negative and the maximum positive enhancement of 4969 mT (DNP(-)) and 4980 mT (DNP(+)), respectively. However, the indirect process yields a maximum enhancement at high-field (DNP(+)), whereas for direct ^{13}C polarization the maximum enhancement is observed at low-field (DNP(-)). The origin of the asymmetry is likely due to the size of the nuclear Larmor frequencies (211 MHz for ^1H , 53 MHz for ^{13}C at 5 T) relative to the large g- and hyperfine anisotropy (600 MHz) of the TEMPO moieties. In particular, to satisfy the CE matching condition for ^1H , the separation of the spin packets in the EPR spectrum must be spaced by 211 MHz, yet the maximum in the spin packet intensity distribution of the EPR powder pattern occurs to the low field side of g_{yy} (see Figure 1). Therefore, the maximum enhancement is to the high field side at ~ 4980 mT. In contrast, for ^{13}C polarization the EPR spin packets only need to be spaced by 53 MHz, and that difference fits nicely within the g_{xx} - g_{yy} region of the

lineshape. Thus, the largest enhancement for the direct process is on the low field side of the EPR spectrum. The behavior seems to be an intrinsic feature of TEMPO-based polarizing agents [16,17] and numerical simulations are currently in progress to provide a more complete understanding.

A potential advantage of polarizing nuclei other than ^1H is the larger enhancement available due to a larger ratio of the magnetic moments. The theoretical maximum enhancement for DNP is given by the ratio γ_S/γ_I of the electron (S) and nuclear (I) gyromagnetic ratio (660 for $e^-/^1\text{H}$ and 2640 for $e^-/^{13}\text{C}$). Indeed, we observe a two-fold larger enhancement from direct polarization of ^{13}C (Table 1). However, a significant disadvantage of polarizing nuclei other than ^1H is that the time constant for the polarization build up, τ_B , becomes much longer. This is illustrated in Figure 2 for direct ^{13}C polarization of samples with different ^{13}C concentrations. Each sample contained 10 mM TOTAPOL as the polarizing agent and the bulk-polarization build-up curves are measured at a field position corresponding to DNP(+). A field position corresponding to DNP(-) produced the same results (data not shown).

At a temperature of 90 K, τ_B depends strongly on the ^{13}C concentration and values ranging from 114 to 176 s were measured. For ^1H τ_B is typically ~ 5 s, a factor of 23–37 shorter. The experimental build-up constants and enhancement factors are summarized in Table 1.

At a given temperature, several factors influence τ_B , the concentration of the polarizing agent, and the concentration of the spins that are polarized. The influence of the electron concentration on τ_B is easy to understand. If the electron concentration is increased, each electron has to polarize fewer nuclei and τ_B decreases. However, the concentration of the bulk spins has a direct influence on the efficiency of the spin-diffusion process, while the identity of the DNP process (SE or CE) has no or only a negligible influence on τ_B , because τ_B is a bulk property. Since ^1H nuclei, even when they are magnetically dilute, still experience a strong inter-nuclear dipole interaction, we observe only a small variation of the ^1H τ_B (Table 1). In fact the ^1H concentration must be optimized to obtain the maximum signal enhancements.[15,19] This is different for ^{13}C nuclei. Here, the spin-diffusion process is dramatically attenuated by the lower gyromagnetic ratio of ^{13}C and the ^{13}C concentration. Even for the largest ^{13}C concentration that can be achieved, τ_B^{C} is more than factor 20 larger than τ_B^{H} (see Table 1). In addition for biological samples internal dynamics of the protein can drastically influence the ^1H longitudinal relaxation times (e.g. rotational tunnelling of methyl groups) and therefore τ_B . However, all measurements presented here were performed in a glycerol/water matrix, which forms a rigid glass at 90 K. In more complex samples (e.g. bio-macromolecules) these relaxation effects can be addressed by deuteration of the sample and the matrix. [15,19]

Very long microwave polarization times were required for the dissolution experiment developed by the Malmoe group. [20,21] Our studies indicate that this is due to the slow propagation of polarization among ^{13}C , reflecting the smaller dipolar coupling between these nuclei and to the distant electron as well as the low temperature at which polarization occurs (< 1.4 K). Moreover, to exploit the full benefits of dissolution-DNP, the polarization time has to be of the order of $5*\tau_B$ (full steady-state polarization) because the experimental cycle cannot be repeated. In contrast, in an indirect DNP experiment τ_B is much shorter, due to the larger intermolecular ^1H dipolar coupling. Furthermore, since the polarization process can be repeated, the experiment can be performed at an optimum repetition rate ($t_{\text{mw}} = 1.26*\tau_B$), to achieve the maximum enhancement per unit time. Therefore our studies indicate that it is more efficient in a DNP-enhanced MAS experiment to initially polarize ^1H nuclei and then transfer this polarization to ^{13}C via cross-polarization.

In summary we demonstrate that direct ^{13}C polarization yields more than 2-fold larger enhancements than ^1H polarization combined with subsequent cross-polarization step to ^{13}C . Furthermore, the optimal field for direct DNP of ^{13}C is on the low rather than the high field side of the EPR spectrum. However, due to the smaller dipolar coupling mediating spin-diffusion, the time constant for polarization build up is significantly longer, making direct ^{13}C polarization experiments much slower, as is observed for dissolution experiments. In contrast, initial ^1H polarization followed by a subsequent CP step can be incorporated into a dissolution experiment with the simple addition of a multiple resonance probe. In this case the shorter ^1H build-up times can be exploited, by pumping the polarization from the electrons to the ^{13}C nuclei through the ^1H spin reservoir. This would significantly decrease the polarization times required in a dissolution experiment.

Experimental Section

Sample preparation

DNP samples were prepared from a mixture of glycerol/ $^2\text{H}_2\text{O}$ (60/40 w/w) with different ratios of [$^{12}\text{C}_3$]- and [$^{13}\text{C}_3$] glycerol as indicated in the text. The TOTAPOL concentration was 10 mM for all samples.

DNP experiments

DNP experiments were performed on a custom designed 211 MHz DNP/NMR spectrometer using a triple-resonance cryogenic 2.5 mm MAS probe (e^- , ^1H , and ^{13}C) with a commercial stator (Revolution NMR Inc.). The spectrometer operates at a magnetic field of 5 T, corresponding to a Larmor frequency of 140 GHz for e^- . High-power microwave radiation ($> 10\text{ W}$) is generated by a gyrotron, operating at a frequency of 139.662 GHz.[22–24]. The NMR magnet is equipped with a superconducting sweep coil that allows field sweeps over $\pm 750\text{ G}$. For accurate field measurements the spectrometer is equipped with a field/frequency lock system.[25] All experiments were performed at 90 K at a spinning frequency $\omega_r/2\pi = 5\text{ kHz}$ and 100 kHz TPPM[26] decoupling. The ^1H and ^{13}C field strengths used for cross-polarization and decoupling were typically 50 kHz.

Acknowledgments

This research was supported by the National Institutes of Health through grants EB002804 and EB002026. T.M. acknowledges receipt of a postdoctoral fellowship from the Deutsche Forschungsgemeinschaft. AFM acknowledges financial support by the Office of the Vice President for Research, University of Kentucky.

References

1. Abragam A, Goldman M. Rep. Prog. Phys. 1978; 41:395–467.
2. Carver TR, Slichter CP. Physical Review. 1953; 92:212.
3. Höfer P, Carl P, Guthausen G, Prisner T, Reese M, Carlomagno T, Griesinger C, Bennati M. Appl. Magn. Reson. 2008; 34:393–398.
4. Barnes AB, De Paëpe G, van der Wel PCA, Hu KN, Joo CG, Bajaj VS, Mak-Jurkauskas ML, Sirigiri JR, Herzfeld J, Temkin RJ, Griffin RG. Appl. Magn. Reson. 2008; 34:237–263. [PubMed: 19194532]
5. Maly T, Debelouchina GT, Bajaj VS, Hu K-N, Joo C-G, MakJurkauskas ML, Sirigiri JR, van der Wel PCA, Herzfeld J, Temkin RJ, Griffin RG. J. Chem. Phys. 2008; 128:052211–052219. [PubMed: 18266416]
6. Goertz ST. Nucl. Instrum. Methods Phys. Res., Sect. A. 2004; 526:28–42.
7. Gallagher FA, Kettunen MI, Day SE, Hu D-E, Ardenkjaer-Larsen JH, Zandt R i t, Jensen PR, Karlsson M, Golman K, Lerche MH, Brindle KM. Nature. 2008; 453:940–943. [PubMed: 18509335]

8. Atsarkin VA. *Sov. Phys. Usp.* (english translation). 1978; 21:725–743.
9. Hu K, Bajaj V, Rosay M, Griffin R. *J Chem Phys.* 2007; 126:044512. [PubMed: 17286492]
10. Wollan DS. *Phys. Rev. B.* 1976; 13:3686.
11. Wollan DS. *Phys. Rev. B.* 1976; 13:3671.
12. N. Bloembergen *Physica.* 1949; 15:386–426.
13. Pines A, Gibby MG, Waugh JS. *J. Chem. Phys.* 1972; 56:1776–1777.
14. Pines A, Gibby MG, Waugh JS. *J. Chem. Phys.* 1973; 59:569–590.
15. Song C, Hu K, Joo C, Swager T, Griffin R. *J. Am. Chem. Soc.* 2006; 128:11385–11390. [PubMed: 16939261]
16. Matsuki Y, Maly T, Ouari O, Karoui H, Moigne Le F, Rizzato E, Lyubenova S, Herzfeld J, Prisner TF, Tordo P, Griffin RG. *Angew. Chem. Int. Ed.* 2009; 48:4996–5000.
17. Hu K-N, Song C, Yu H-h, Swager TM, Griffin RG. *J. Chem. Phys.* 2008; 128:052302–052317. [PubMed: 18266419]
18. Gerfen GJ, Becerra LR, Hall DA, Griffin RG, Temkin RJ, Singel DJ. *J. Chem. Phys.* 1995; 102:9494–9497.
19. Kagawa A, Murokawa Y, Takeda K, Kitagawa M. *J. Magn. Reson.* 2009; 197:9–13. [PubMed: 19091611]
20. Ardenkjær-Larsen J, Fridlund B, Gram A, Hansson G, Hansson L, Lerche M, Servin R, Thaning M, Golman K. *Proc Natl Acad Sci U S A.* 2003; 100:10158–10163. [PubMed: 12930897]
21. Reynolds S, Patel H. *Appl. Magn. Reson.* 2008; 34:495–508.
22. Becerra L, Gerfen G, Temkin R, Singel D, Griffin R. *Phys. Rev. Lett.* 1993; 71:3561–3564. [PubMed: 10055008]
23. Becerra LR, Gerfen GJ, Bellew BF, Bryant JA, Hall DA, Inati SJ, Weber RT, Un S, Prisner TF, McDermott AE, Fishbein KW, Kreisler K, Temkin RJ, Singel DJ, Griffin RG. *J. Magn. Reson.* 1995; A117:28–40.
24. Granatstein VL, Parker RK, Armstrong CM. *Proc. IEEE.* 1999; 87:702–716.
25. Maly T, Bryant J, Ruben D, Griffin R. *J. Magn. Reson.* 2006; 183:303–307. [PubMed: 17027306]
26. Bennett AE, Rienstra CM, Auger M, Lakshmi KV, Griffin RG. *J. Chem. Phys.* 1995; 103:6951–6958.

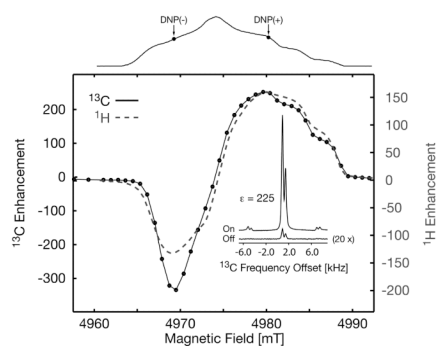


Figure 1. ^1H and ^{13}C DNP-enhancement profile for TOTAPOL. The corresponding 140 GHz EPR spectrum is shown at the top. The inset shows a representative ^{13}C spectrum of $^{13}\text{C}_3$ -glycerol, with and without DNP (direct ^{13}C polarization). $T = 90\text{ K}$, $\omega_{\text{R}}/2\pi = 5\text{ kHz}$.

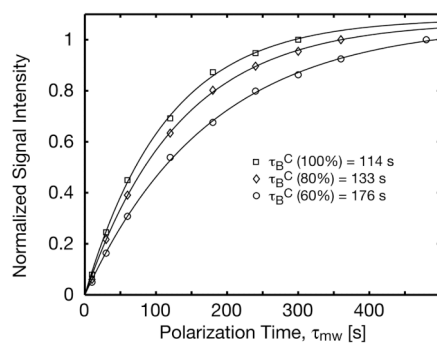


Figure 2.
 ^{13}C direct polarization. Bulk-polarization build-up times τ_B for different ^{13}C concentrations.
 $T = 90 \text{ K}$, $\omega_R/2\pi = 5 \text{ kHz}$.

Table 1Polarization build-up times τ_B and enhancements ϵ^H for ^1H and ^{13}C polarization

^{13}C	τ_B^H [S]	$\epsilon_+^H(\epsilon_-^H)$	τ_B^C [S]	$\epsilon_+^C(\epsilon_-^C)$
100 % (22.2/7.4) ^[a]	5.3	130 (108)	114	225 (281)
80 % (17.7/5.9)	5.2	150 (125)	133	253 (316)
60 % (13.2/4.4)	4.8	154 (128)	176	244 (305)

^[a]Fraction in [%] of $^{13}\text{C}_3$ glycerol in $^{12}\text{C}_3$ glycerol. Total ^{13}C concentration (1st number) and glycerol concentration (2nd number) in M for the 60/40 glycerol/ $^2\text{H}_2\text{O}$ mixture. For build-up constants an error of <5 % was estimated. For enhancement factors the error is ~10 %, dominated by the poor signal-to-noise ratio of the off-signal.